Bull Math Biol (2011) 73:1881–1908
DOI 10.1007/s11538-010-9596-2

ORIGINAL ARTICLE

The Evolution of Virulence in RNA Viruses under a Competition–Colonization Trade-Off

Edgar Delgado-Eckert · Samuel Ojosnegros · Niko Beerenwinkel

Received: 14 January 2010 / Accepted: 15 October 2010 / Published online: 17 November 2010

Abstract RNA viruses exist in large intra-host populations which display great genotypic and phenotypic diversity. We analyze a model of viral competition between two viruses infecting a constantly replenished cell pool. We assume a trade-off between the ability of the virus to colonize new cells (cell killing rate or virulence) and its local competitiveness (replicative success within coinfected cells). We characterize the conditions that allow for viral spread by means of the basic reproductive number and show that a local coexistence equilibrium exists, which is asymptotically stable. At this equilibrium, the less virulent competitor has a reproductive advantage over the more virulent colonizer reflected by a larger equilibrium population size of the competitor. The equilibria at which one virus outcompetes the other one are unstable, i.e., a second virus is always able to permanently invade. We generalize the two-virus model to multiple viral strains, each displaying a different virulence. To account for the large phenotypic diversity in viral populations, we consider a continuous spectrum of virulences and present a continuum limit of this multiple viral strains model that describes the time evolution of an initial continuous distribution of virulence without mutations. We provide a proof of the existence of solutions of the model equations, analytically assess the properties of stationary solutions, and present numerical approximations of solutions for different initial distributions. Our simulations suggest that initial continuous distributions of virulence evolve toward a distribution that is extremely skewed in favor of competitors. At equilibrium, only the least virulent part of the population survives. The discrepancy of this finding in the continuum limit with the two-virus model is attributed to the skewed equilibrium subpopulation sizes and to the transition to a continuum. Consequently, in viral quasispecies with high

E. Delgado-Eckert (✉) · S. Ojosnegros · N. Beerenwinkel
Department of Biosystems Science and Engineering, ETH Zurich, Mattenstrasse 26, 4058 Basel, Switzerland
e-mail: edgar.delgado-eckert@mytum.de

E. Delgado-Eckert · N. Beerenwinkel
Swiss Institute of Bioinformatics, Basel, Switzerland

virulence diversity, the model predicts collective virulence attenuation. This result may contribute to understanding virulence attenuation, which has been reported in several experimental studies.

Keywords SIR models of viral infection · Competition–colonization dynamics · RNA virus · Evolution of virulence · Attenuation of virulency

1 Introduction

RNA viruses are fast evolving pathogens that can adapt to continuously changing environments. Due to their error-prone replication, large population size, and high turnover, RNA virus populations exist as quasispecies (Eigen et al. 1988; Holland et al. 1992; Domingo and Holland 1997). The viral mutant spectrum consists of many genetic variants which give rise to diverse phenotypes. This phenotypic diversity is reflected in different traits, including the rate of killing host cells, which is referred to as virulence herein.

The concept of virulence has been used in various areas of the life sciences with different meanings. In evolutionary biology, the virulence of a pathogen is defined as the fitness costs to the host that are induced by the pathogen. In epidemiology, the term usually means the pathogen-induced host mortality. In clinical settings, virulence often refers to the severity of disease symptoms induced by a pathogen. In this article, we consider intra-host virus dynamics and use the term virulence to denote the cell killing rate of a virus infecting tissue. Thus, we apply the epidemiological meaning of virulence to the intra-host viral microepidemics. This definition is related to the macroscopic or inter-host concept of virulence, because, in general, the cell killing rate of a virus affects the course of infection and the mortality of the host.

The evolution of virulence has been studied using experimental and theoretical approaches in a variety of host-pathogen systems and under diverse conditions or assumptions. In the past few decades, the "conventional wisdom" that well-adapted pathogens are avirulent has been replaced by the stricter evolutionary reasoning that successful pathogens exploit their hosts to maximize their number of offspring (Anderson and May 1982; Ewald 1983). In fact, the basic epidemiological model of infection predicts that pathogens will evolve to maximize their basic reproductive number (Nowak 2006). Depending on the specific way how infectivity and virulence are linked in this model, the relationship between pathogens and their hosts can range from commensalism to high pathogenicity (Bremermann and Thieme 1989).

Because pathogens are exposed to different environmental conditions during their life cycle, they face different types of selective pressure, and adaptation is typically controlled by various phenotypic traits that are not independent. In order to investigate the constraints of adaptability and their impact on the evolution of virulence, several adaptive trade-off theories have been proposed (Bull 1994; Frank 1996). These models assume finite resources and make an economic argument by trading off two or more pathogen traits. For example, the trade-off between rapid pathogen reproduction (virulence) and longer transmission time due to longer life time of the host is often considered (Bremermann and Thieme 1989; Bonhoeffer et al. 1996; Cooper et al. 2002). The virulence-transmission trade-off can

give rise to intermediate or increased virulence, but Lenski and May (1994) have argued that intermediate virulence levels can lead to reduced virulence in the long run.

Multilevel selection models address the trade-off between pathogen competition within and among hosts. Krakauer and Komarova (2003) find intermediate virulence levels when modeling an intracellular trade-off between genome replication capacity and genetic translation applied to polio virus. Coombs et al. (2007) integrate the evolutionary and ecological processes of infection and study within- versus between-host competition and find that the strain that maximizes between-host fitness dominates. In the presence of mutation, coexistence is possible, and distributions of diverse virulence values with complex dynamics have been observed (Bonhoeffer and Nowak 1994; Coombs et al. 2007; Boldin and Diekmann 2008). Diverse distributions of virulence are also predicted by a superinfection model without coinfection, but with a hierarchy of competitive dominance among strains (Nowak and May 1994; May and Nowak 1994). In this model, the average virulence increases, and highly virulent strains can be maintained in the population.

The superinfection model of May and Nowak (1994) is closely related to the metapopulation model of Tilman (1994), in which coexistence results from spatially structured habitats. A trade-off between the ability of each individual to colonize unoccupied territory and to compete with others for the same habitat patch can result in coexistence of two strategies, competition and colonization. Competitors have an advantage when competing locally for resources, whereas colonizers are more successful in reaching new resources.

Competition–colonization dynamics have recently been demonstrated in an RNA virus *in vitro* using an experimental and theoretical approach (Ojosnegros et al. 2010a, 2010b). In this system, highly virulent viral strains play the role of colonizers, because they kill cells faster and thus replicate faster, which allows faster spread and colonization of new cells. Local competition arises when two or more different viruses infect the same cell and compete for intracellular resources. Competitors manage to produce more offspring in a cell coinfected together with a colonizer and, at the same time, extend the cell killing time characteristic of a colonizer, a phenomenon known as viral interference.

The competition–colonization coevolutionary dynamics of two different viral strains in cell culture have been described in Ojosnegros et al. (2010a) by a modification of the basic model of virus dynamics (Nowak and May 2000a; Perelson and Nelson 1999). The model predicts that the outcome of viral competition for the cell monolayer depends on the initial overall number of viruses per cell. Under low initial density, colonizers produce more total offspring, whereas under high density conditions, coinfection is more likely to occur, and hence competitors have a selective advantage. This prediction was confirmed experimentally.

In the present article, we make a first step toward transferring the results obtained *in vitro* to the *in vivo* situation under the assumption of a competition–colonization trade-off. We extend the basic model of competition–colonization dynamics of two different viral strains in cell culture by replacing the finite cell monolayer with a constantly replenished pool of uninfected cells. Furthermore, to account for the postulated competition–colonization trade-off, we archetypically model the intracellular fitness of the viruses during coinfection as being inversely proportional to their respective virulence. Like any adaptive trade-off theory, our model is a metaphor for

host-pathogen systems that highlights a specific aspect of the evolution of virulence, namely the interplay between competition and colonization strategies (Frank 1996).

We present a rigorous analytical study of this model and demonstrate that it allows for local asymptotically stable coexistence of competitors and colonizers. Moreover, the less virulent competitor is shown to have a reproductive advantage reflected by its higher abundance and a higher number of cells infected with it at equilibrium.

We generalize this model by considering more than two viral variants. We assume that different viral strains can only be distinguished through their virulences and ask how a distribution of virulences is modified in the course of the infection by the competition–colonization dynamics. In other words, we study the time evolution of a distribution of virulences. While simulation results for a finite number of viral strains will be presented elsewhere (Ojosnegros et al., in preparation), here we account for the high phenotypic diversity of RNA virus populations by considering the continuum limit of this multiple-viral-strain model. In the continuum limit, we consider a continuous interval of virulence values and model the time evolution of a continuous distribution of virulence. We provide a proof of the existence of solutions of this model's equations, analytically assess the properties of stationary solutions, and present numerical approximations.

Our simulations suggest that initial continuous distributions of virulence evolve toward a distribution which is heavily skewed in favor of competitors such that, eventually, only the least virulent part of the population will survive. This finding is in contrast to the coexistence equilibrium of the two-virus model. It is a consequence of the transition to a continuum and the skewed subpopulation sizes at equilibrium. Thus, the competition–colonization model predicts attenuation of the virus population. This result might explain previous observations of suppression of high-fitness mutants in various viral systems (De la Torre and Holland 1990; Novella et al. 2004; Turner and Chao 1999; Bull et al. 2006).

This article is organized as follows. In Sect. 2, we formulate the basic model of two competing viral strains and illustrate our model assumptions. In the Results section, a detailed analytical study of its equilibrium behavior is presented. In Sect. 3.5, the multiple-viral-strain model is introduced, and in Sect. 3.6, we derive its continuum limit. The continuous-virulence model is analyzed both analytically and numerically. We close in Sect. 4 by discussing some of the model assumptions and consequences for the evolution of virulence. The supplementary material can be obtained from the corresponding author upon request via email.

2 Formulation of the Two-Viral-Strain Model

Our modeling approach is based on the basic SIR model of virus dynamics (Nowak and May 2000b; Perelson and Nelson 1999), which we extend in order to model two different viral populations giving rise to singly infected and doubly infected or coinfected cells. It is well known that cells infected with a virus can be significantly modified and no longer follow the normal biochemical processes. In particular, an infected cell is transformed into a new living organism that has its own death process. This new death process defines the average death rate of a population of infected cells, i.e., the virulence a of the infecting viral strain. In the case of coinfected cells we assume that the new death rate is imposed by the less virulent infecting strain (see

Box below). Accordingly, the time evolution of the concentration of two competing viral strains, uninfected and infected cells, is described by the following system of ordinary differential equations:

$$\begin{aligned}
\dot{x} &= \lambda - dx - \beta x(v_1 + v_2) \\
\dot{y}_1 &= \beta x v_1 - \beta y_1 v_2 - a_1 y_1 \\
\dot{y}_2 &= \beta x v_2 - \beta y_2 v_1 - a_2 y_2 \\
\dot{y}_{12} &= \beta(y_1 v_2 + y_2 v_1) - \min(a_1, a_2) y_{12} \\
\dot{v}_1 &= K a_1 y_1 + cK \min(a_1, a_2) y_{12} - u v_1 \\
\dot{v}_2 &= K a_2 y_2 + (1-c) K \min(a_1, a_2) y_{12} - u v_2
\end{aligned} \tag{1}$$

The variable x models the concentration of uninfected cells with an external constant supply of new cells at rate λ, dying at a rate d and being infected with efficiency β. The variables v_1 and v_2 describe the concentration of strain 1 and strain 2, respectively. The variable y_i represents the concentration of cells infected solely with strain i. These cells die and release viral offspring at rate a_i, the virulence of strain i. The variable y_{12} models the concentration of cells infected with both viral strains. These cells die and release viral offspring at rate $\min(a_1, a_2)$ (more on this below). Free virus of type i is produced at rate $k_i = K a_i$, where K is the burst size, and inactivated at rate u. The parameter c denotes the proportion of strain 1 produced at the burst of coinfected cells. The state of the system at time t is denoted by $S(t) = (x(t), y_1(t), y_2(t), y_{12}(t), v_1(t), v_2(t))^T$.

We make the following general assumptions about the parameters:

- All parameters are positive.
- The efficiency with which strain 1 respectively strain 2 infects uninfected cells or singly infected cells is equal and denoted by β.
- The death rates of strain 1 and strain 2 are equal and denoted by u.

Furthermore, based on the experimental results presented in Ojosnegros et al. (2010a), see Box below, we assume:

- The burst size of singly and coinfected cells is equal and denoted by K.
- The death rate a_{12} of coinfected cells is equal to the death rate of cells singly infected with the least virulent virus, i.e., $a_{12} = \min(a_1, a_2)$. In other words, this rate is imposed by the least virulent viral strain.
- To account for the competition–colonization trade-off postulated, we model the intracellular fitness of the viruses during coinfection as being inversely proportional to their respective virulence by setting $c := a_1^{-1}/(a_1^{-1} + a_2^{-1})$. In this archetypical form of a trade-off, we capture the assumption that poor colonization abilities are compensated by intracellular competition abilities and vice versa.

Without loss of generality, we can assume that $a_1 \leq a_2$. Thus, strain 1 is the better competitor, while strain 2 is the better colonizer, and the last three equations of (1) become

$$\begin{aligned}
\dot{y}_{12} &= \beta y_1 v_2 + \beta y_2 v_1 - a_1 y_{12} \\
\dot{v}_1 &= K a_1 y_1 + cK a_1 y_{12} - u v_1 \\
\dot{v}_2 &= K a_2 y_2 + (1-c) K a_1 y_{12} - u v_2
\end{aligned}$$

In Ojosnegros et al. (2010a), the model (1) with $\lambda = 0$, $d = 0$, $a_1 < a_2$, and an unconstrained (i.e., independent of a_1) parameter $c > 1/2$ was introduced to describe two competing viral strains in cell culture. These special in vitro conditions of a fixed and limited amount of target cells allowed for an analytical treatment of the system in the large initial virus load limit which is not possible in the more general case of system (1) considered here.

Ojosnegros et al. (2010a) described the diversification of a single purified clone of foot-and-mouth disease virus into two populations that resembled the ecological strategies of competition and colonization.
The phenotype of the two strategies showed the following main features:

- Colonizers are virulent variants with higher cell killing rate.
- Competitors kill the cells slower than colonizers, but when competitors and colonizers infect the same cell, the cell dies as slowly as if infected only by competitors.
- Competitors and colonizers show identical progeny production, that is, the same burst size.
- Competitors produce more progeny in coinfected cells: When a cell is coinfected with both variants, the production of each variant is uneven, and competitors are favored.
- Because of the different replication capacity during independent infections or during coinfections, the competition–colonization strategies follow a density-dependent selection. Under low density of viruses, coinfections are rare, many cells are available, and colonizers spread faster. Under high density of viruses, coinfections are frequent, and competitors have an advantage.

3 Results

3.1 Establishing Infection

To identify the conditions on the parameters of the model that imply spread of at least one of the viral strains, we analyze the stability of the (obvious) equilibrium point

$$S^{(0)} = \left(x^{(0)}, y_1^{(0)}, y_2^{(0)}, y_{12}^{(0)}, v_1^{(0)}, v_2^{(0)}\right)^T := (\lambda/d, 0, 0, 0, 0, 0)^T$$

at which the infection dies out. The Jacobian matrix J of system (1) evaluated at $S^{(0)}$ is

$$J(S^{(0)}) = \begin{pmatrix} -d & 0 & 0 & 0 & -\beta\lambda/d & -\beta\lambda/d \\ 0 & -a_1 & 0 & 0 & \beta\lambda/d & 0 \\ 0 & 0 & -a_2 & 0 & 0 & \beta\lambda/d \\ 0 & 0 & 0 & -a_1 & 0 & 0 \\ 0 & Ka_1 & 0 & cKa_1 & -u & 0 \\ 0 & 0 & Ka_2 & (1-c)Ka_1 & 0 & -u \end{pmatrix}$$

The eigenvalues of this matrix are

$$-d, \quad -a_1, \quad \frac{-d(a_i+u)+\Delta_i}{2d}, \quad \frac{-d(a_i+u)-\Delta_i}{2d}, \quad i=1,2,$$

where $\Delta_i := \sqrt{d^2(a_i-u)^2+4Ka_i\beta\lambda d}$ for $i=1,2$. All eigenvalues are real given that all parameters are assumed to be positive. This equilibrium becomes unstable as soon as at least one eigenvalue is positive. This happens if and only if $-d(a_1+u)+\Delta_1>0$ or $-d(a_2+u)+\Delta_2>0$, which is equivalent to $d(a_1-u)^2+4Ka_1\beta\lambda > d(a_1+u)^2$ or $d(a_2-u)^2+4Ka_2\beta\lambda > d(a_2+u)^2$. The latter expression is in turn equivalent to $K\beta\lambda > du$. In other words, it is generically sufficient for viral spread that

$$R_0 := \frac{K\beta\lambda}{du} > 1 \tag{2}$$

For generic parameter values (the fine tuning $K\beta\lambda = du$ cannot be expected), this condition is also necessary, because $K\beta\lambda < du$ implies that $S^{(0)}$ is asymptotically stable.

If we consider initial conditions in which $y_i(0)=0,\ y_{12}(0)=0,\ v_i(0)=0$, and $v_j(0)\neq 0$, where $i,j\in\{1,2\}, i\neq j$, the model reduces to a simple SIR model of single viral infection (Bonhoeffer et al. 1997; Nowak and May 2000b; Korobeinikov 2004), and we recognize the magnitude R_0 as the well-known *basic reproductive number* of the infection system. Condition (2) can also be expressed as $M := K\beta\lambda - du > 0$. The magnitude M turns out to be algebraically very helpful for our further analysis of the model.

Having determined a condition on the parameter values that characterizes viral spread, we next ask whether under these circumstances, the system admits a steady state in which both viral strains can coexist. The opposite steady state scenario would be that one of the viral strains outcompetes the other. To this end, we examine further fixed points of the system and their stability.

3.2 Further Fixed Points

Performing algebraic manipulations we found the following nontrivial fixed points of system (1):

$$S^{(1)} = \begin{pmatrix} x^{(1)} \\ y_1^{(1)} \\ y_2^{(1)} \\ y_{12}^{(1)} \\ v_1^{(1)} \\ v_2^{(1)} \end{pmatrix} := \frac{1}{\beta}\begin{pmatrix} u/K \\ M/(a_1K) \\ 0 \\ 0 \\ M/u \\ 0 \end{pmatrix}, \qquad S^{(2)} = \begin{pmatrix} x^{(2)} \\ y_1^{(2)} \\ y_2^{(2)} \\ y_{12}^{(2)} \\ v_1^{(2)} \\ v_2^{(2)} \end{pmatrix} := \frac{1}{\beta}\begin{pmatrix} u/K \\ 0 \\ M/(a_2K) \\ 0 \\ 0 \\ M/u \end{pmatrix}$$

and

$$S^* = \begin{pmatrix} x^* \\ y_1^* \\ y_2^* \\ y_{12}^* \\ v_1^* \\ v_2^* \end{pmatrix} := \frac{1}{\beta K} \begin{pmatrix} u \\ a_2 u M/(a_1(M + u(a_1 + a_2))) \\ a_1 u M/(a_2(M + u(a_1 + a_2))) \\ M^2/(a_1(M + u(a_1 + a_2))) \\ a_2 K M/(u(a_1 + a_2)) \\ a_1 K M/(u(a_1 + a_2)) \end{pmatrix}$$

By the assumed positivity of the parameters and by $M > 0$ (we assume that viral spread is possible) all these fixed points are (component-wise) nonnegative and thus biologically meaningful. We also found a fourth fixed point S^- which, nevertheless, has negative entries for all parameter values considered. Summarizing, we have two equilibria, $S^{(1)}$ and $S^{(2)}$, in which one of the viral strains outcompetes the other, and one coexistence equilibrium S^*. The following subsections are devoted to studying their properties.

3.3 The Coexistence Equilibrium

The Jacobian matrix $J(S^*)$ of system (1) evaluated at the equilibrium point S^* equals

$$\begin{pmatrix} -\beta\lambda K/u & 0 & 0 & 0 & -u/K & -u/K \\ \frac{a_2 M}{u(a_1+a_2)} & -\frac{a_1 M}{u(a_1+a_2)} - a_1 & 0 & 0 & u/K & -\frac{a_2 u M}{a_1 K(M+u(a_1+a_2))} \\ \frac{a_1 M}{u(a_1+a_2)} & 0 & -\frac{a_2(M+u(a_1+a_2))}{u(a_1+a_2)} & 0 & -\frac{a_1 u M}{a_2 K(M+u(a_1+a_2))} & u/K \\ 0 & \frac{a_1 M}{u(a_1+a_2)} & \frac{a_2 M}{u(a_1+a_2)} & -a_1 & \frac{a_1 u M}{a_2 K(M+u(a_1+a_2))} & \frac{a_2 u M}{a_1 K(M+u(a_1+a_2))} \\ 0 & K a_1 & 0 & \frac{K a_1 a_2}{(a_1+a_2)} & -u & 0 \\ 0 & 0 & K a_2 & \frac{K a_1^2}{(a_1+a_2)} & 0 & -u \end{pmatrix}$$

The characteristic polynomial of this matrix is too long to be displayed here. Thus, we performed its analysis using computer algebra and symbolic computation. Under the premise of viral spread, i.e., $M > 0$, we used the computer algebra system Maple™ to show that all coefficients are positive. Furthermore, we used Maple™ to construct Routh's table (reviewed in Barnett and Šiljak 1977) and verified that all entries in its first column are positive (see supplementary material). By Routh's criterion (reviewed in Barnett and Šiljak 1977), all roots of the characteristic polynomial have strictly negative real parts. As a consequence, the equilibrium point S^* in which both viral strains can coexist is a local asymptotically stable fixed point. This holds for all positive parameter values, provided that $M > 0$.

The peculiarity of this coexistence equilibrium is that the viral load at equilibrium of the competitor, $v_1^* = a_2 M/(\beta u(a_1 + a_2))$, is proportional to the *relative* virulence of the colonizer. Similarly, the viral load at equilibrium of the colonizer, $v_2^* = a_1 M/(\beta u(a_1 + a_2))$, is proportional to the relative virulence of the competitor. Thus, the two-viral-strain system (1) not only allows for coexistence of both viral strains, but it confers the less virulent competitor a reproductive advantage over the more virulent colonizer. This discrepancy is reflected in the higher concentration of

competitors, $v_1^*/v_2^* = a_2/a_1 > 1$, and the higher concentration of cells infected with competitors, $y_1^*/y_2^* = (a_2/a_1)^2 > 1$, at equilibrium.

To analyze which features of the model are responsible for the peculiar properties of the coexistence equilibrium, we consider the two major model assumptions, namely the competition–colonization trade-off, $c = a_1^{-1}/(a_1^{-1} + a_2^{-1})$, and the cell killing rate imposed by competitors in coinfected cells, i.e., the factor $\min(a_1, a_2)$ in the last three equations of model (1). The second assumption turns out to be not crucial, which can be seen as follows. If we replace the minimum in model (1) by the maximum and assume that $a_1 \leq a_2$ as before, then we obtain

$$\begin{aligned}
\dot{y}_{12} &= \beta(y_1 v_2 + y_2 v_1) - a_2 y_{12} \\
\dot{v}_1 &= K a_1 y_1 + c K a_2 y_{12} - u v_1 \\
\dot{v}_2 &= K a_2 y_2 + (1-c) K a_2 y_{12} - u v_2
\end{aligned}$$

for the last three equations, while all others remain unchanged. Comparing this model to the original one, we realize that strain 1 and strain 2 have interchanged their roles so that the equation for strain 1 now has mixed virulence terms whereas the one for strain 2 has become homogeneous. In other words, we might as well write the maximum model as

$$\begin{aligned}
\dot{x} &= \lambda - dx - \beta x(v_1 + v_2) \\
\dot{y}_2 &= \beta x v_2 - \beta y_2 v_1 - a_2 y_2 \\
\dot{y}_1 &= \beta x v_1 - \beta y_1 v_2 - a_1 y_1 \\
\dot{y}_{12} &= \beta y_1 v_2 + \beta y_2 v_1 - a_2 y_{12} \\
\dot{v}_2 &= K a_2 y_2 + \widetilde{c} K a_2 y_{12} - u v_2 \\
\dot{v}_1 &= K a_1 y_1 + (1-\widetilde{c}) K a_2 y_{12} - u v_1
\end{aligned}$$

where $\widetilde{c} := a_2^{-1}/(a_1^{-1} + a_2^{-1})$. This model is equivalent to (1) with a_1 and a_2 having switched their roles. The coexistence equilibrium in the maximum model is

$$\begin{pmatrix} x^* \\ y_2^* \\ y_1^* \\ y_{12}^* \\ v_2^* \\ v_1^* \end{pmatrix} = \frac{1}{\beta K} \begin{pmatrix} u \\ a_1 u M/(a_2(M + u(a_2 + a_1))) \\ a_2 u M/(a_1(M + u(a_2 + a_1))) \\ M^2/(a_2(M + u(a_2 + a_1))) \\ a_1 M K/(u(a_2 + a_1)) \\ a_2 M K/(u(a_2 + a_1)) \end{pmatrix}$$

at which competitors and cells infected with competitors are more abundant, $v_1^*/v_2^* = a_2/a_1 > 1$ and $y_1^*/y_2^* = (a_2/a_1)^2 > 1$.

We have compared the effect of the cell killing rate of coinfected cells on the steady state by testing the smallest and the largest values that are biologically plausible, namely, $\min(a_1, a_2)$ and $\max(a_1, a_2)$. We argue that any value in between (i.e.,

$a_{12} \in (\min(a_1, a_2),\ \max(a_1, a_2)))$ would not make a qualitative difference. Simulation results not presented here support this conjecture. Therefore, the comparison of the minimum and the maximum models lets us conclude: (1) How two different viral strains "compromise" within a coinfected cell regarding the cell killing velocity does not affect the steady state properties of the two-viral-strain model, and (2) the crucial property is the inverse proportionality between virulence and intracellular fitness during coinfection. The functional shape $c = a_1^{-1}/(a_1^{-1} + a_2^{-1})$ of this trade-off is likely to play an important role (see Discussion).

3.4 Single Viral Strain Equilibria

The existence of a local asymptotically stable coexistence equilibrium suggests that a viral strain can bear the presence of another one. However, to fully address the question of whether system (1) always allows for a second viral strain to invade tissue already infected with a different strain, we examine the stability of the equilibria $S^{(1)}$ and $S^{(2)}$, in which one of the viral strains ousts the other.

The Jacobian matrix of system (1) evaluated at the point $S^{(1)}$ is

$$J(S^{(1)}) = \begin{pmatrix} -M/u - d & 0 & 0 & 0 & -u/K & -u/K \\ M/u & -a_1 & 0 & 0 & u/K & -M/(a_1 K) \\ 0 & 0 & -\frac{M}{u} - a_2 & 0 & 0 & u/K \\ 0 & 0 & M/u & -a_1 & 0 & M/(a_1 K) \\ 0 & K a_1 & 0 & K a_1 a_2/(a_1 + a_2) & -u & 0 \\ 0 & 0 & K a_2 & K a_1^2/(a_1 + a_2) & 0 & -u \end{pmatrix}$$

Assuming viral spread ($M > 0$), we showed using Maple™ that the leading coefficient of the characteristic polynomial of $J(S^{(1)})$ is positive, whereas the independent coefficient is negative (see supplementary material). By Routh's criterion, at least one root of the characteristic polynomial has positive real part. Therefore, the equilibrium point $S^{(1)}$ in which the competitor outcompetes the colonizer is not stable. Analogously, we found that the equilibrium point $S^{(2)}$ in which the colonizer outcompetes the competitor is also unstable. Both statements hold for all positive parameter values, provided that $M > 0$.

However, it is worth mentioning that any trajectory $S(t)$ for which one viral strain, say of type i, and all cells infected or coinfected with it have disappeared at some point in time s would stay confined in the corresponding hyperplane $H_i := \{(x, y_1, y_2, y_{12}, v_1, v_2)^T \mid y_i = y_{12} = v_i = 0\}$ for all $t \geq s$. As mentioned in Sect. 3.1, *within* the corresponding hyperplanes, the equilibria $S^{(1)}$ and $S^{(2)}$ become asymptotically stable, provided that $R_0 > 1$. Whether a trajectory starting outside H_i flows into the hyperplane or not remains to be analytically studied. Our simulations do not show any evidence for this type of behavior.

3.5 Multiple-Viral-Strains Model

A straightforward generalization of our model (1) that accounts for the experimentally observed diversity of viral populations is to consider more than two competing

viral strains. This generalization raises the question of how many viruses can coinfect a cell simultaneously. For example, the multiplicity of HIV-infected spleen cells has been reported between 1 and 8 with mean 3.2 (Jung et al. 2002). However, for the sake of mathematical simplicity, we consider here the case in which at most two viruses can coinfect a cell. We assume that we can distinguish each of the viral strains via their corresponding virulences a_i. As above, we assume inverse proportionality between virulence and intracellular fitness during coinfection. In other words, the proportion of strain i produced at the burst of a cell coinfected with strains i and j is given by $c_i := a_i^{-1}/(a_i^{-1} + a_j^{-1})$ for all $i, j \in \{1, \ldots, n\}$, $i < j$, where $n \in \mathbb{N}$ is the total number of viral strains modeled. Thus, the equations for the generalized model read

$$\dot{x} = \lambda - dx - \beta x \sum_{j=1}^{n} v_j$$

$$\dot{y}_i = \beta x v_i - \beta y_i \left(\sum_{\substack{j=1 \\ j \neq i}}^{n} v_j \right) - a_i y_i, \quad i = 1, \ldots, n$$

$$\dot{y}_{lj} = \beta(y_l v_j + y_j v_l) - \min(a_l, a_j) y_{lj}, \quad l, j = 1, \ldots, n \text{ and } l < j$$

$$\dot{v}_i = K a_i y_i + a_i^{-1} K \left(\sum_{\substack{l,j \\ l<j}} \frac{1}{a_l^{-1} + a_j^{-1}} w_i(l, j) \min(a_l, a_j) y_{lj} \right) - u v_i, \quad i = 1, \ldots, n$$

where $w_i(l, j) = 1$ if $l = i$ or $j = i$, and otherwise $w_i(l, j) = 0$. The model does not explicitly account for the order of infection. Nevertheless, to increase the symmetry of the model and to simplify the notation, we will consider the order of infection events and separately model the populations y_{lj} and y_{jl}, where the order of the indices indicates the order of infection with the viral strains l and j. With this notation, in general, $y_{lj} \neq y_{jl}$, and the variable y_{12} in the two-viral-strain model (1) refers to $y_{12} + y_{21}$. To be consistent, we have to make sure that for $l \neq j$, the magnitude $y_{lj} + y_{jl}$ obeys the corresponding equation, that is,

$$\dot{y}_{lj} + \dot{y}_{jl} = \beta(y_l v_j + y_j v_l) - \min(a_l, a_j)(y_{lj} + y_{jl})$$

To ensure this, the equation for y_{lj} becomes

$$\dot{y}_{lj} = \beta y_l v_j - \min(a_l, a_j) y_{lj}, \quad l, j = 1, \ldots, n \text{ s.t. } l \neq j$$

Summarizing, we obtain the following model:

$$\begin{aligned} \dot{x} &= \lambda - dx - \beta x \sum_{j=1}^{n} v_j \\ \dot{y}_i &= \beta x v_i - \beta y_i \left(\sum_{\substack{j=1 \\ j \neq i}}^{n} v_j \right) - a_i y_i, \quad i = 1, \ldots, n \end{aligned} \tag{3}$$

$$\dot{y}_{lj} = \beta y_l v_j - \min(a_l, a_j) y_{lj}, \quad l, j = 1, \ldots, n \text{ s.t. } l \neq j$$

$$\dot{v}_i = K a_i y_i + a_i^{-1} \left(\sum_{\substack{j=1 \\ j \neq i}}^{n} \frac{1}{a_i^{-1} + a_j^{-1}} K \min(a_i, a_j)(y_{ij} + y_{ji}) \right) - u v_i, \quad i = 1, \ldots, n$$

Note that the magnitude $\sum_{j=1}^{n} v_j(t)$ is the total viral population at any given point in time t.

Since the number of equations in this model grows quadratically with the number n of viral strains, it becomes rather involved to analyze it. In Ojosnegros et al. (in preparation) the results of numerical simulation for numerically tractable values of n are presented. Here, in compliance with the quasispecies view of viral populations, we devise a new approach to studying the evolution of virulence and consider the continuum limit of the multistrain model (3). In this continuum limit, we consider a continuous spectrum of virulence values and identify viral strains with virulence values. We call the resulting continuum limit the continuous-virulence model. In this model, the viral quasispecies is represented by a time-dependent continuous distribution of virulence. Unlike the discrete multiple-viral-strains model, the continuum approach allows us to study the virulence distribution of diverse RNA virus populations in a manner independent of the number of different strain types.

3.6 Continuous-Virulence Model

We identify viral strains with their virulence a and denote by $v(a, t)$ the density of viruses of type a at time t. If we consider an interval $[a_1, a_2] \subset (0, 1)$ of possible virulences (defined and justified in the next subsection), then the initial distribution of virulences is defined by a continuous density function $v(\cdot, 0) : \mathbb{R} \to \mathbb{R}$ which vanishes outside the interval $[a_1, a_2]$. The continuum limit of model (3) is therefore the following integro-differential (Cushing 1977) initial-value problem (also known as Cauchy problem):

$$\begin{aligned}
\dot{x}(t) &= \lambda - d x(t) - \beta x(t) \int_{a_1}^{a_2} v(\xi, t)\, d\xi \\
\frac{\partial y}{\partial t}(a, t) &= \beta x(t) v(a, t) - \beta y(a, t) \left(\int_{a_1}^{a_2} v(\xi, t)\, d\xi \right) - a y(a, t) \\
\frac{\partial z}{\partial t}(a, b, t) &= \beta y(a, t) v(b, t) - \min(a, b) z(a, b, t) \\
\frac{\partial v}{\partial t}(a, t) &= K a y(a, t) + a^{-1} K \left(\int_{a_1}^{a_2} \frac{1}{a^{-1} + b^{-1}} \min(a, b)(z(a, b, t) \right. \\
&\qquad \left. + z(b, a, t))\, db \right) - u v(a, t) \\
x(0) &= x_0, \qquad y(\xi, 0) = y_0(\xi), \qquad z(\vartheta, \mu, 0) = z_0(\vartheta, \mu) \\
v(\xi, 0) &= v_0(\xi)
\end{aligned} \tag{4}$$

For every $t \in \mathbb{R}_{\geq 0}$, the function $z(\cdot, \cdot, t) : [a_1, a_2] \times [a_1, a_2] \to \mathbb{R}$ describes the density of coinfected cells with respect to the two-dimensional Lebesgue measure on $\mathbb{R}^2$.

Table 1 Parameters of the model of evolution of virulence during infection. These values were chosen based on the measurements underpinning Ojosnegros et al. (2010a)

Parameter	Description	Value	Units
λ	Natural growth rate of uninfected population	10^5	$(\text{ml}\cdot\text{h})^{-1}$
d	Natural death rate of uninfected population	0.05	h^{-1}
β	Rate of infection	$5 \cdot 10^{-8}$	ml/h
K	Burst size	150	dimensionless
u	Clearance rate of free virus	0.15	h^{-1}

The value $z(a, b, t)$ is only meaningful for our modeling purposes outside the diagonal $a = b$. Note that the exception $j \neq i$ in the sums of the original discrete model can be neglected here because the values of a real-valued function on a set of measure zero do not modify the value of the integral.

In Appendix A we provide a proof of the existence of solutions of system (4).

3.6.1 Simulation Results

In order to explore the dynamics of the continuous-virulence model, we numerically solved the Cauchy problem (4), as described in Appendix B, using typical parameter values given in Table 1. Because y, z, and v represent concentration densities, the units of y and v are [concentration]/[virulence], and the unit of z is [concentration]/[virulence]^2. Given that the unit of virulence is [Time]$^{-1}$, y, z, and v are measured in units of [Time]/[Volume], [Time]^2/[Volume], and [Time]/[Volume], respectively. The variable x represents a concentration, and its unit is therefore [Volume]$^{-1}$.

As stated in Sect. 2, cells infected with a virus are significantly modified and no longer follow the normal biological processes. As a consequence, compared to populations of uninfected cells, populations of infected cells display a different death rate, (i.e., the virulence of the infecting viral strain).

By definition, a death rate must be positive; thus, we have a first lower bound for possible values of virulence, namely zero. Moreover, the question arises as to whether the death rate of infected cells (i.e., the virulence of the infecting virus) can become lower than the natural death rate of uninfected cells. In the case of oncogenic viruses, this might be possible under certain circumstances; however, we do not intend to consider this type of scenario here. In conclusion, we assume that the virulence is bounded from below by d, the natural death rate of uninfected cells.

We set the upper limit of the interval of possible virulence values to $1/2\ \text{h}^{-1}$ based on general knowledge about how fast RNA viruses can kill a cell and experimental observations, see García-Arriaza et al. (2006).

The aforementioned lower and upper bounds of virulence imply that, within the framework of our model, the distribution of virulence in a viral population has to be confined to the interval $[a_1, a_2] := [d, 0.5]$. In other words, the support of any virulence distribution must lie within $[d, 0.5]$.

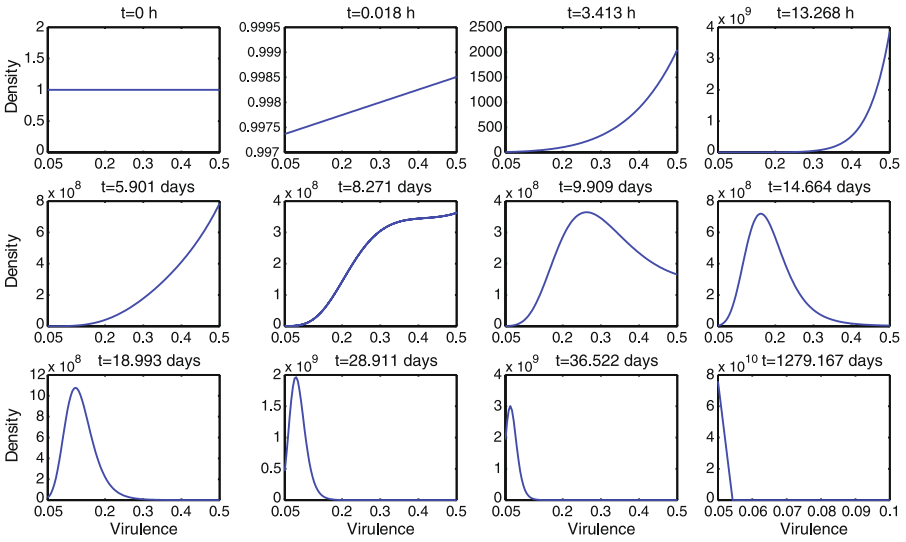

Fig. 1 Time evolution of a uniform initial distribution of virulences. Each panel shows the shape of the density function at the point in time displayed in its title

Starting from non infected tissue, i.e., $x_0 = \lambda/d$, $y_0(\xi) \equiv 0$, and $z_0(\vartheta, \mu) \equiv 0$, we studied three different initial *unnormalized* continuous distributions of virulences given by the densities $v(a, 0) = v_0(a)$, $a \in [d, 0.5]$:

1. A uniform distribution defined by $v_0(a) = \mathbf{1}_{[d,0.5]}(a)$, where $\mathbf{1}_{[d,0.5]}$ is the indicator function of the set $[d, 0.5]$. The total initial concentration is given by $\int_{\mathbb{R}} v_0(a)\,da = \int_d^{0.5} v_0(a)\,da = 0.450\ \text{ml}^{-1}$.
2. A truncated Gaussian distribution with mean value $\mu = 1/4$ and standard deviation $\sigma = 1/40$ given by $v_0(a) = \mathbf{1}_{[d,0.5]}(a)e^{-800(a-1/4)^2}$. The total initial concentration is given by $\int_{\mathbb{R}} v_0(a)\,da = \int_d^{0.5} v_0(a)\,da \approx 0.063\ \text{ml}^{-1}$.
3. A truncated mixture of two Gaussian distributions with mean values $\mu_1 = 1/6$, $\mu_2 = 4/10$, equal standard deviations $\sigma_1 = \sigma_2 = 1/150$, and unequal weights $\lambda_1 = 3/10$ and $\lambda_2 = 7/10$ given by $v_0(a) = \mathbf{1}_{[d,0.5]}C((3/7)e^{-11250(a-1/6)^2} + (7/10)e^{-11250(a-4/10)^2})$, where C is a constant. The total initial concentration is given by $\int_{\mathbb{R}} v_0(a)\,da = \int_d^{0.5} v_0(a)\,da \approx 0.024\ \text{ml}^{-1}$.

The time evolution of a flat initial virulence density is shown in snapshots in Fig. 1. After a very short absorption phase, the density takes an exponential shape in favor of the most virulent part of the interval which is greatly amplified during the first 13 hours of simulation time. After approximately 14 hours a recession is observed, which by $t = 5.9$ days has already decreased the populations' density by one order of magnitude. After approximately 8 days a qualitative change takes place, and the distribution starts loosing its exponential shape to become a nonsymmetric unimodal distribution with mode around a virulence of $0.275\ \text{h}^{-1}$ at $t = 9.9$ days. This distribution starts traveling to the left, becomes narrower and more symmetric. By $t = 19$ days the distribution has moved further to the left and is now almost symmetric. At

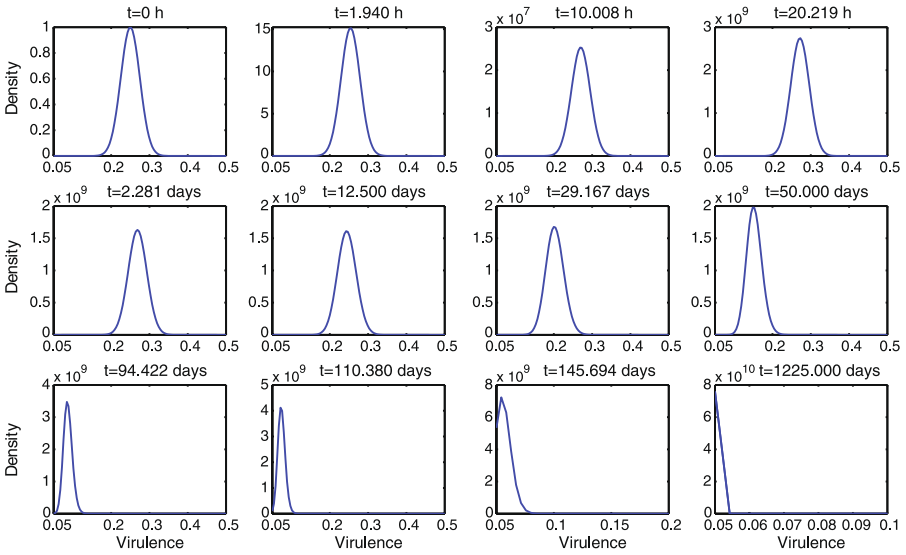

Fig. 2 Time evolution of a Gaussian initial distribution of virulences

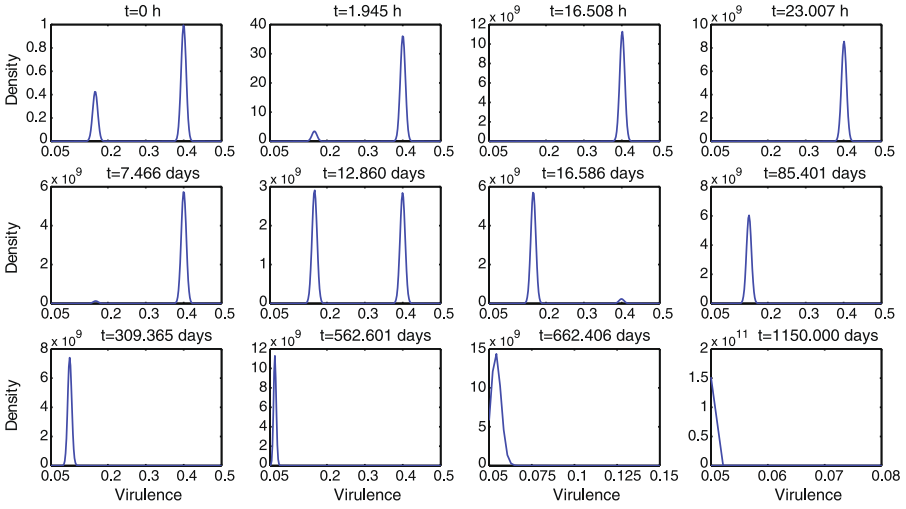

Fig. 3 Time evolution of a Gaussian mixture initial distribution of virulences

this point, the dynamics become significantly slower, and we start observing an amplification effect. At $t = 29$ days the distribution starts changing its shape to become an exponentially shaped distribution, this time in favor of low-virulence competitors. The changes become very slow, and, at least numerically, the system seems to be reaching a stationary distribution highly in favor of the smallest virulence values. (In the supplementary material we provide movies of the simulations depicted by snapshots in Figs. 1, 2, and 3.)

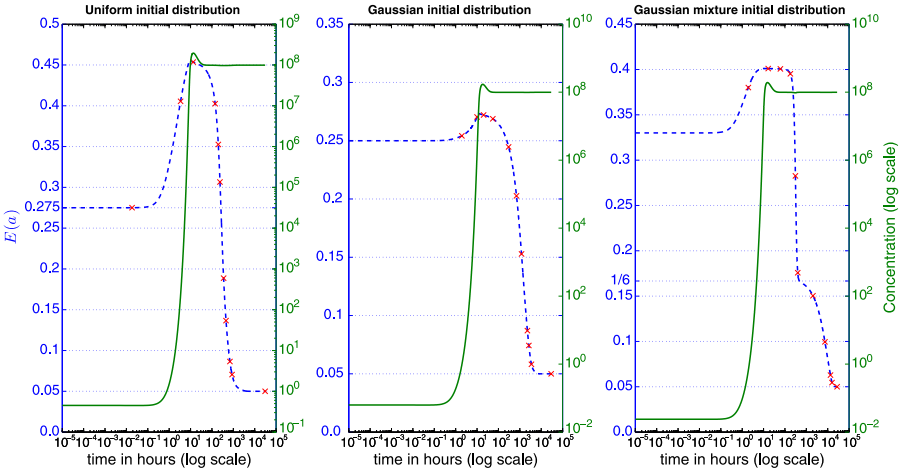

Fig. 4 Time evolution of the expected value $E(a)(t) = \int_{a_1}^{a_2} \xi v(\xi, t)/\|v(b,t)\|\, d\xi$ of virulence (dashed curve, vertical axes on the left) and of the total concentration of viruses $\int_{a_1}^{a_2} v(b,t)\, db$ (solid curve, vertical axes on the right) for three different initial distributions. The crosses mark the value of $E(a)$ at the time points (>0) depicted in the corresponding evolution-of-distribution-figure (Figs. 1–3)

Despite the prominent differences between the initial distributions, Figs. 2 and 3 reveal similar qualitative properties of the dynamics, namely, a biphasic behavior comprising an initial phase in which the more virulent parts of the density are amplified, followed by a second phase in which the less virulent regions predominate. All three trajectories become very similar once the density becomes unimodal, although the time scales are significantly different, and all three reach very similar numerically stationary distributions (see the following subsection).

We also experimented with an initial virulence density derived from the truncated mixture of two Gaussians described above, namely, the same density except for the fact that it vanishes at a distance of seven standard deviations left and right from each of the means μ_1 and μ_2. More precisely, the density vanishes on the intervals $[d, \mu_1 - 7\sigma_1]$, $[\mu_1 + 7\sigma_1, \mu_2 - 7\sigma_2]$, and $[\mu_2 + 7\sigma_2, 1/2]$. The numerical simulation (see movie in the supplementary material) reveals dynamics very similar to the ones depicted in Fig. 3, the main difference being that the exponentially shaped distribution observed at the onset of numerical stationarity is located to the right of the cut-off point $\mu_1 - 7\sigma_1$ instead of d.

For each of the three initial virulence densities $v_0(a)$ listed above, Fig. 4 shows the time evolution of the expected value $E(a)$ of the virulence at point in time t, $E(a)(t) = \int_{a_1}^{a_2} \xi v(\xi, t)/\|v(b,t)\|\, d\xi$, which is obtained by normalizing with[1] $\|v(b,t)\| := \int_{a_1}^{a_2} |v(b,t)|\, db$ at each point in time t, as the system of integro-partial differential equations is not norm-preserving. Figure 4 also depicts the time evolution of the total concentration of viruses $\int_{a_1}^{a_2} v(b,t)\, db = \|v(b,t)\|$. In this graph, we can clearly identify the two different regimes of the biphasic behavior described above.

[1] $\|f\| := \int_{a_1}^{a_2} |f(x)|\, dx$ is indeed a norm in the space $\mathbf{L}_1([a_1, a_2])$.

This biphasic behavior can also be observed in simulations of the two-viral-strain model (simulations presented in Ojosnegros et al., in preparation). As a matter of fact, the simulations suggest that the coexistence equilibrium (see Sect. 3.3) is globally attracting, provided that $M > 0$. If we assume that this equilibrium is globally attracting under the premise of viral spread ($M > 0$), we can conclude that starting from initial conditions in which the most virulent virus predominates ($v_2(0) > v_1(0)$), the system must undergo this biphasic behavior. On the other hand, starting from initial conditions in which the least virulent virus predominates ($v_1(0) > v_2(0)$), the differential equations for the viral populations at an early stage in which the number of coinfected cells can be neglected can be written as

$$\dot{v}_1 = K a_1 y_1 - u v_1$$
$$\dot{v}_2 = K a_2 y_2 - u v_2$$

Thus, at an early stage, the population v_2 of the most virulent virus grows faster than the population v_1 of the least virulent one. Depending on the initial values $v_1(0)$ and $v_2(0)$, the most virulent virus might or might not become more numerous than the least virulent one during the initial phase.

3.6.2 Analytical Assessment of Stationary Solutions

Given the apparent convergence observed in our three simulation experiments, we speculated whether the exponentially shaped distribution observed toward the end of the simulations would become steeper and steeper and eventually stabilize as the (Dirac) delta distribution δ_{a_1} with peak at $a = a_1$. To explore this hypothesis, we formulated the following ansatz for the stationary distributions:

$$\begin{aligned} y^*(a) &= Y \delta_{a_1}(a) \\ v^*(a) &= V \delta_{a_1}(a) \\ z^*(a,b) &= Z \delta_{(a_1,a_1)}(a,b) \end{aligned} \tag{5}$$

where δ_{a_1} is the one-dimensional delta distribution centered at a_1, $\delta_{(a_1,a_1)}$ is the two-dimensional delta distribution centered at (a_1, a_1), and $Y, V, Z \in \mathbb{R}$ are parameters to be determined. For the x component, the stationary value is just a point $x^* \in \mathbb{R}$, a fourth parameter to be determined. In order to obtain conditions that determine these four parameters, we assume that the solution postulated in (5) is stationary, that is, the right-hand side of (4) should vanish in a distributional sense. The first equation of (4) yields (recall that $\int_{\mathbb{R}} \delta_{a_1}(\xi)\, d\xi = \int_{a_1}^{a_2} \delta_{a_1}(\xi)\, d\xi = 1$)

$$\lambda - d x^* - \beta x^* V = 0 \tag{6}$$

The second and third equations of (4) yield

$$\beta x^* V \delta_{a_1}(a) - \beta Y \delta_{a_1}(a) V - a Y \delta_{a_1}(a) = 0$$
$$\beta Y \delta_{a_1}(a) V \delta_{a_1}(a) - \min(a,b) Z \delta_{(a_1,a_1)}(a,b) = 0$$

These are to be understood in a distributional sense, that is, for any test function F with support contained in $[a_1, a_2]$, it should hold (recall that $\delta_{a_1}(F) = \int_{\mathbb{R}} \delta_{a_1}(\xi) F(\xi)\, d\xi = F(a_1)$)

$$\begin{aligned}
&\big(\beta x^* V \delta_{a_1}(a) - \beta Y \delta_{a_1}(a) V - aY\delta_{a_1}(a)\big)(F) \\
&\quad = \int_{\mathbb{R}} \big(\beta x^* V \delta_{a_1}(a) - \beta Y \delta_{a_1}(a) V - aY\delta_{a_1}(a)\big) F(a)\, da \\
&\quad = \int_{a_1}^{a_2} \big(\beta x^* V \delta_{a_1}(a) - \beta Y \delta_{a_1}(a) V - aY\delta_{a_1}(a)\big) F(a)\, da \\
&\quad = \beta x^* V F(a_1) - \beta Y V F(a_1) - a_1 Y F(a_1) = 0
\end{aligned}$$

Analogously, for any test function F with support contained in $[a_1, a_2] \times [a_1, a_2]$, we require

$$\begin{aligned}
&\big(\beta Y \delta_{a_1}(a) V \delta_{a_1}(b) - \min(a,b) Z \delta_{(a_1,a_1)}(a,b)\big)(F) \\
&\quad = \int_{\mathbb{R}^2} \big(\beta Y \delta_{a_1}(a) V \delta_{a_1}(b) - \min(a,b) Z \delta_{(a_1,a_1)}(a,b)\big) F(a,b)\, da\, db \\
&\quad = \int_{a_1}^{a_2} \int_{a_1}^{a_2} \big(\beta Y \delta_{a_1}(a) V \delta_{a_1}(b) - \min(a,b) Z \delta_{(a_1,a_1)}(a,b)\big) F(a,b)\, da\, db \\
&\quad = \beta Y V F(a_1, a_1) - a_1 Z F(a_1, a_1) = 0
\end{aligned}$$

In particular, for a function F with $F(a_1) \neq 0$, it holds

$$\beta x^* V - \beta Y V - a_1 Y = 0 \tag{7}$$

And analogously, for a function F with $F(a_1, a_1) \neq 0$, we have

$$\beta Y V - a_1 Z = 0 \tag{8}$$

By the same distributional argument, for any test function F with support contained in $[a_1, a_2]$, the fourth equation of (4) yields

$$\begin{aligned}
&\Bigg(KaY\delta_{a_1}(a) + a^{-1} K \Bigg(\int_{a_1}^{a_2} \frac{1}{a^{-1} + b^{-1}} \min(a,b) Z(\delta_{(a_1,a_1)}(a,b) \\
&\qquad + \delta_{(a_1,a_1)}(b,a))\, db \Bigg) - uV\delta_{a_1}(a) \Bigg)(F) \\
&\quad = \int_{a_1}^{a_2} KaY\delta_{a_1}(a) F(a)\, da + K \Bigg(\int_{a_1}^{a_2} \int_{a_1}^{a_2} \frac{a^{-1}}{a^{-1} + b^{-1}} \min(a,b) Z(\delta_{(a_1,a_1)}(a,b) \\
&\qquad + \delta_{(a_1,a_1)}(b,a)) F(a)\, db\, da \Bigg) - \int_{a_1}^{a_2} uV\delta_{a_1}(a) F(a)\, da \\
&\quad = Ka_1 Y F(a_1) + Ka_1 Z F(a_1) - uV F(a_1) = 0
\end{aligned}$$

Again, for a function F with $F(a_1) \neq 0$, we have

$$Ka_1Y + Ka_1Z - uV = 0 \tag{9}$$

Summarizing, the stationarity argument has provided us with a system of four nonlinear equations (6), (7), (8), and (9) for the unknown parameters x^*, Y, Z, and V. By solving this system of equations algebraically we obtain

$$L^{(0)} = \begin{pmatrix} x^{(0)} \\ Y^{(0)} \\ Z^{(0)} \\ V^{(0)} \end{pmatrix} := \begin{pmatrix} \lambda/d \\ 0 \\ 0 \\ 0 \end{pmatrix}$$

and

$$L^* = \begin{pmatrix} x^* \\ Y^* \\ Z^* \\ V^* \end{pmatrix} := \frac{1}{\beta K} \begin{pmatrix} u \\ uM/(M + ua_1) \\ M^2/(a_1(M + ua_1)) \\ KM/u \end{pmatrix}$$

where $M = K\beta\lambda - du$ as before.

The solution $L^{(0)}$ represents the state in which the infection dies out. Interestingly, if we simulate the continuous-virulence model using parameters such that the condition for viral spread established for the two-viral-strain model is not fulfilled (i.e., $M < 0$), the system evolves toward this state (results not explicitly shown).

The solution L^* has a remarkable structural similarity with the coexistence solution S^* we found for the two-viral-strain model. However, the corresponding stationary solution cannot be regarded as a coexistence solution, because only the least virulent part of the population survives. The stationarity argument presented above was strongly validated when we confirmed that in each of the three simulation experiments presented in the previous subsection the following holds:

$$\begin{aligned} x(T) &= x^* \\ \int_{a_1}^{a_2} y(\xi, T)\, d\xi &= Y^* \\ \int_{a_1}^{a_2} \int_{a_1}^{a_2} z(\xi, \eta, T)\, d\xi\, d\eta &\approx Z^* \\ \int_{a_1}^{a_2} v(\xi, T)\, d\xi &= V^* \end{aligned}$$

where T is the total simulation time run.

This concordance provides strong evidence for the convergence of our simulations toward a stationary solution of (4). There is a small discrepancy in the case of the integral of $z(\xi, \eta, T)$ over $[a_1, a_2] \times [a_1, a_2]$. We attribute this discrepancy to the discretization error that arises during the numerical approximation of the integral using an equidistant grid on $[a_1, a_2] \times [a_1, a_2]$.

With the parameter values L^* obtained, our ansatz (5) leads us to a nontrivial stationary solution of (4). While this solution seems to be the point of convergence of our simulations, it would go beyond the scope of this article to analytically assess its (local) stability properties.

4 Discussion

We have analyzed the evolution of virulence of an RNA viral quasispecies in which the cell killing capacity (the virulence a_i) of viruses is inversely related to the intracellular viral fitness within coinfected cells. In the case of two viral strains, this competition–colonization trade-off allows for stable coexistence of competitors and colonizers, and each virus type can be invaded by the other. This holds for all positive parameter values, provided that the conditions for viral spread are given ($M > 0$). These conditions do not depend on the particular virulence values a_i. However, the population levels at the coexistence equilibrium do depend on the particular virulence values a_i, and this dependency is in favor of the least virulent viral strain. Moreover, as substantiated at the end of Sect. 3.6.1, the dynamics of this two-strain system show a biphasic behavior comprising an initial phase in which the population of the most virulent strain is more strongly amplified, followed by a second phase in which the population of the least virulent strain predominates.

Generalizing this two-viral-strain model to multiple viral strains is conceptually straightforward, but the resulting system of differential equations is difficult to study analytically. Moreover, the lack of accurate experimental measurements of the actual number of (in terms of virulence) different strains contained in a viral population limits the applicability of this modeling approach. Furthermore, the quadratic dependency of the number of equations on the number of strains n constrains the dimension of the models that can be numerically analyzed (Kryazhimskiy et al. 2007). We circumvented these issues by considering a continuous spectrum of virulence values and introducing a model that describes the time evolution of a continuous distribution of virulences under the same type of competition–colonization trade-off. This model is naturally derived as the continuum limit of the multiple-viral-strain model, providing a better modeling framework for the high phenotypic diversity of viral populations. While the model exhibits a complicated mathematical structure as an integro-differential Cauchy problem, we were able to provide a simple proof of the existence of solutions. We solved the Cauchy problem numerically using typical parameter values. The discretization step size in the numerical scheme (see Appendix B) clearly limits the accuracy of the numerical approximations. However, this numerical limitation does not represent a loss of modeling power, whereas computational complexity does limit the number of scenarios that can be modeled using the discrete multiple-strain model.

Our simulation results indicate that the intra-host evolution of virulence is characterized by two phases. During the first phase, colonizers become more frequent, and the average virulence of the population increases. In the second phase, the abundance of competitors increases, and the mean population virulence decreases. Eventually, the virulence distribution takes an exponential shape in favor of the least virulent part

of the population. In our simulations, this distribution seems to be converging towards $V\delta_{a_1}$, where δ_{a_1} is the delta distribution centered at a_1, and $V \in \mathbb{R}$ is a suitable constant. However, convergence takes infinite time, implying that, after a finite period of time (in our simulations ranging from 1 month to 1.8 years), the exponentially shaped distribution in favor of the least virulent part of the population becomes the qualitatively characteristic state of the intra-host viral population.

We assumed that the virulence is bounded from below by d, the natural death rate of uninfected cells, and bounded from above by 0.5. Accordingly, in the three simulations presented above we considered initial distributions of virulence with probability density functions that are positive in the interval $[a_1, a_2] = [d, 0.5]$ and zero otherwise. However, we have observed in other simulations (one example is provided as a movie in the supplementary material) that the statements of the previous paragraph also hold for initial distributions of virulence with support $[a_1, a_2]$ satisfying $[a_1, a_2] \subset (d, 0.5]$. This observation suggests that our conclusions regarding the steady state of the system are not dependent on the particular virulence value displayed by the least virulent strain represented in the initial viral population.

As mentioned in Sect. 3.6.2, we made the interesting observation that if we simulate the continuous-virulence model using parameters such that the condition for viral spread is not fulfilled (i.e., $M < 0$), the system evolves toward the zero density function (results not shown). This outcome seems to be independent of the initial distributions of virulence used. This result suggests that the condition for viral spread, which we originally derived for the two-viral-strain model, appears to be still valid in the continuum limit. This finding raises the general question of the similarities and differences between the qualitative properties of the dynamics displayed by both models. We saw that the dynamics of both models show the biphasic behavior described above and that the requirements for viral spread seem to be the same. On the other hand, there is an important difference between the models: While all simulations of the two-viral-strain model we have run converge to the coexistence equilibrium S^*, the simulations of the continuum limit model seem to be converging toward a weighted delta distribution centered at a_1, in other words, toward a distribution that only allows for the existence of the least virulent strain of the initial population. The explanation for this phenomenon lies in the skewed equilibrium abundances of the viral subpopulations of different virulence and is highlighted in simulations of the discrete model (3).

We ran simulations of this model (results presented in Ojosnegros et al., in preparation) with increasing values of the number n of viral strains, whose corresponding virulence values were uniformly distributed over the interval $[a_1, a_2]$. Analogously to the simulations presented in Sect. 3.6.1, the initial abundances of each viral strain obeyed uniform, Gaussian, and Gaussian mixture distributions, respectively. We observed that these simulations converge to an exponentially shaped discrete distribution in favor of the least virulent strains in the initial population. With an increasing number of viral strains, this steady-state discrete distribution becomes steeper and steeper, and some of the most virulent strains become extinct. In other words, at steady state, coexistence is only possible among the less virulent strains.

In view of this observation, the stationary behavior displayed by the continuum limit model (4) can be understood as the limit case for $n \to \infty$ of the steady-state

distribution displayed by the discrete model (3). The similarities in the simulations of models (3) and (4) are not surprising, given that the system of ODEs solved to numerically approximate the solution of the continuous virulence system is structurally very similar to the equations of the discrete model, the only difference being the weights that appear in the Newton–Cotes formulas used to approximate the integrals $\int_{a_1}^{a_2} v(\xi, t)\, d\xi$ and $\int_{a_1}^{a_2} \frac{1}{a^{-1}+b^{-1}} \min(a, b)(z(a, b, t) + z(b, a, t))\, db$ (see Appendix B).

It is well known that RNA viruses replicate with high error rates (see, for instance, Domingo 2006). We can not discard that mutation plays a role in modulating the evolution of virulence, although in this initial study we have considered a more simplified scenario. The main outcome of our simulation study, namely the imposition of competitors over colonizers after a transient domination by the colonizers, seems to be independent of the initial shape of the distribution of virulence. Thus, we expect that mutations altering the distribution of virulence might delay the convergence toward a stationary distribution by resetting the dynamic process. Accordingly, we conjecture that the steady state may occur in the form of a dynamic polymorphism of virulent variants, similar to the one described by the quasispecies model (Eigen 1971; Eigen et al. 1988). However, the byphasic behavior of the competition–colonization model might still hold after implementation of mutation mechanisms. Moreover, we speculate that very high mutational rates could yield an oscillatory behavior in which the predominance of colonizers and of competitors alternates.

In conclusion, the two models studied in this article make two major predictions about the evolution of virulence under a competition–colonization trade-off. First, two viral strains with distinct virulence can coexist, and second, a viral population displaying a range of virulence values will be attenuated and evolve toward a population of many competitors and very few colonizers. Our model predictions differ from those of other epidemiological models of infection which predict that selection maximizes the basic reproductive number of the pathogen. This discrepancy is due to the following model assumptions: (1) We introduce specific variables and equations to model the populations of coinfected cells, (2) we do not assume that the viral strain with the highest individual cell killing performance dominates the events during coinfections, and (3) we assume a competition–colonization trade-off.

Under these assumptions, selection appears to favor low-virulence competitors, as long as uninfected cells are constantly replenished, but not unlimited. The attenuation property of the continuous-virulence model may also explain experimental observations of suppression of high-fitness viral mutants (colonizers), which might have been displaced by competitors (De la Torre and Holland 1990; Novella et al. 2004; Turner and Chao 1999; Bull et al. 2006) and intra-host virulence attenuation events (Sanz-Ramos et al. 2008).

In Ojosnegros et al. (2010a) two foot-and-mouth disease viral strains were reported that had been isolated from a population undergoing viral passaging experiments (see also Box above). Measurement of cell killing rates, intracellular fitness, and other parameters suggested a competition–colonization trade-off. These experimental findings motivated the hypothesis that viruses can specialize

either to improve colonization by fast cell killing or to improve competitive intracellular reproductive success. In our modeling approach, we have implemented the competition–colonization trade-off using the algebraically simple relationship $c = a_1^{-1}/(a_1^{-1} + a_2^{-1})$, which renders the mathematical analysis convenient. The actual dependency between virulence a_i and intracellular fitness c is likely to be more complicated and to depend on additional parameters. It would be of biological interest to identify and to characterize virus populations with a competition–colonization trade-off and to establish the nature of the trade-off experimentally.

Acknowledgement We would like to thank Dr. Florian Geier for providing very helpful comments on the first draft of the material presented in this article.

The supplementary material can be obtained from the corresponding author upon request via email.

Appendix A: Existence of Solutions of the Continuous-Virulence Model Equations

If we assume that a solution of the initial-value problem (4) exists, then we can derive the following expressions: Setting $V(t) := \int_{a_1}^{a_2} v(\xi, t)\, d\xi$, we have, for the first equation, $\dot{x}(t) = \lambda - dx - \beta x(t) V(t)$ and thus

$$x(t) = \left(x_0 + \int_0^t \lambda e^{W(\xi)}\, d\xi \right) e^{-W(t)} \tag{A.1}$$

where $W(\theta) := \int_0^\theta d + \beta V(\tau)\, d\tau$. The second equation can be solved as

$$y(a,t) = \left(y_0(a) + \beta \int_0^t x(\tau) v(a,\tau) e^{U_a(\tau)}\, d\tau \right) e^{-U_a(t)}$$

where $U_a(\theta) := \int_0^\theta a + \beta V(\tau)\, d\tau$. Substituting the expression for $x(t)$ into the expression for $y(a,t)$ gives

$$\begin{aligned} y(a,t) &= \left(y_0(a) + \beta \int_0^t v(a,\tau) \left(x_0 + \int_0^\tau \lambda e^{W(\xi)}\, d\xi \right) e^{U_a(\tau) - W(\tau)}\, d\tau \right) e^{-U_a(t)} \\ &= \left(y_0(a) + \beta \int_0^t v(a,\tau) \left(x_0 + \int_0^\tau \lambda e^{W(\xi)}\, d\xi \right) e^{(a-d)\tau} d\tau \right) e^{-U_a(t)} \end{aligned} \tag{A.2}$$

The third equation yields

$$z(a,b,t) = \left(z_0(a,b) + \beta \int_0^t y(a,\eta) v(b,\eta) e^{\min(a,b)\eta}\, d\eta \right) e^{-\min(a,b)t} \tag{A.3}$$

Substituting the expression for $y(a,t)$ allows us to express $z(a,b,t) + z(b,a,t)$ in terms of $v(a,\tau)$, $v(b,\tau)$, and integrals involving them as

$$z(a,b,t) + z(b,a,t) = \big(z_0(a,b) + z_0(b,a) + R(a,b,t) \big) e^{-\min(a,b)t}$$

where

$$R(a,b,t) := \beta \int_0^t \Big(\big(v(b,\eta)y_0(a) + v(a,\eta)y_0(b) + Q(a,b,\eta)\big) e^{\min(a,b)\eta - U_a(\eta)} \Big)\, d\eta$$

$$Q(a,b,\eta) := \beta \int_0^\eta \big(v(b,\eta)v(a,\tau)e^{(a-d)\tau} + v(a,\eta)v(b,\tau)e^{(b-d)\tau}\big) \times \left(x_0 + \int_0^\tau \lambda e^{W(\xi)}\, d\xi\right) d\tau$$

Finally, we substitute the expressions obtained for $y(a,t)$ and $z(a,b,t)$ into the differential equation for $v(a,t)$ obtaining

$$\begin{aligned}\frac{\partial v}{\partial t}(a,t) = Ka\Bigg(\Bigg(y_0(a) + \int_0^t \beta v(a,\tau)\Bigg(x_0 + \int_0^\tau \lambda e^{W(\xi)}\, d\xi\Bigg)e^{(a-d)\tau}\, d\tau\Bigg)e^{-U_a(t)}\Bigg) \\ + a^{-1}K\Bigg(\int_{a_1}^{a_2} \frac{1}{a^{-1}+b^{-1}} \min(a,b)\big(z_0(a,b) + z_0(b,a) \\ + R(a,b,t)\big)e^{-\min(a,b)t}\, db\Bigg) - uv(a,t) \qquad \text{(A.4)}\end{aligned}$$

A solution of system (4) necessarily has to fulfill this integro-partial differential equation for the function $v(a,t)$. On the other hand, a solution of the latter equation that is continuous on $[a_1,a_2]\times\mathbb{R}$ and partially differentiable with respect to t and satisfies $v(\xi,0) = v_0(\xi)$ allows for constructing a solution of system (4) by means of substitution of $v(a,t)$ into the expressions (A.1), (A.2), and (A.3).

In order to show that a solution of (4) exists, we consider solutions during a very short time span $[t_1,t_2]\subset[0,\infty)$ within which the values of $V(t)$ and $z(a,b,t)$ do not significantly change, i.e., $V(t)\approx V_{t_1} := V(t_1)$ and $z(a,b,t)\approx z_{t_1}(a,b) := z(a,b,t_1)\ \forall t\in[t_1,t_2]$. Given that (4) is autonomous, we may as well consider the time interval $[t_1=0,t_2]$. Thus, $W(\theta)\approx\int_0^\theta d+\beta V_0\, d\tau = \theta(d+\beta V_0)$, $U_a(\theta)\approx \int_0^\theta a+\beta V_0\, d\tau = \theta(a+\beta V_0)\ \forall\theta\in[0,t_2]$, and $\int_{a_1}^{a_2}\frac{1}{a^{-1}+b^{-1}}\min(a,b)(z(a,b,t)+z(b,a,t))\, db \approx \int_{a_1}^{a_2}\frac{1}{a^{-1}+b^{-1}}\min(a,b)(z_0(a,b)+z_0(b,a))\, db =: S_0(a)\ \forall t\in[0,t_2]$. With this, (A.4) becomes

$$\begin{aligned}\frac{\partial v}{\partial t}(a,t) = Ka\Bigg(y_0(a) + \Bigg(\int_0^t \beta v(a,\tau)\Bigg(x_0 + \lambda\frac{e^{\tau(d+\beta V_0)}-1}{d+\beta V_0}\Bigg) \\ \times e^{(a-d)\tau}\, d\tau\Bigg)e^{-t(a+\beta V_0)}\Bigg) + a^{-1}KS_0(a) - uv(a,t)\end{aligned}$$

where $y_0(a) = y(a,0)$, $x_0 = x(0)$. Some algebra yields

$$\begin{aligned}\frac{\partial v}{\partial t}(a,t) = Ka\Bigg(y_0(a) + \Bigg(\beta\lambda\int_0^t \frac{\beta V_0}{d^2+d\beta V_0}v(a,\tau)e^{(a-d)\tau} \\ + \frac{1}{d+\beta V_0}v(a,\tau)e^{\tau(a+\beta V_0)}\, d\tau\Bigg)e^{-t(a+\beta V_0)}\Bigg)\end{aligned}$$

$$
\begin{aligned}
&+ a^{-1}KS_0(a) - uv(a,t)\\
&= -uv(a,t) + K\beta\lambda a e^{-t(a+\beta V_0)}\\
&\quad\times \int_0^t \left(\frac{\beta V_0}{d^2+d\beta V_0}e^{(a-d)\tau} + \frac{1}{d+\beta V_0}e^{\tau(a+\beta V_0)}\right)v(a,\tau)\,d\tau\\
&\quad + Kay_0(a) + a^{-1}KS_0(a)
\end{aligned}
$$

If we write $e^{-t(a+\beta V_0)}$ as $1+(-a-\beta V_0)t+O(t^2)$ and neglect terms of quadratic order, we obtain, for t sufficiently small,

$$
\begin{aligned}
\frac{\partial v}{\partial t}(a,t) &= -uv(a,t) + K\beta\lambda a\big(1+(-a-\beta V_0)t\big)\\
&\quad\times \int_0^t \left(\frac{\beta V_0}{d^2+d\beta V_0}e^{(a-d)\tau} + \frac{1}{d+\beta V_0}e^{\tau(a+\beta V_0)}\right)v(a,\tau)\,d\tau\\
&\quad + Kay_0(a) + a^{-1}KS_0(a)
\end{aligned}
$$

Let us assume for a moment that a three times differentiable solution exists. Differentiation on both sides yields

$$
\begin{aligned}
\frac{\partial^2 v}{\partial t^2}(a,t) &= -u\frac{\partial v}{\partial t}(a,t) - K\beta\lambda a(a+\beta V_0)\\
&\quad\times \int_0^t \left(\frac{\beta V_0}{d^2+d\beta V_0}e^{(a-d)\tau} + \frac{1}{d+\beta V_0}e^{\tau(a+\beta V_0)}\right)v(a,\tau)\,d\tau\\
&\quad + K\beta\lambda a\big(1+(-a-\beta V_0)t\big)\\
&\quad\times \left(\frac{\beta V_0}{d^2+d\beta V_0}e^{(a-d)t} + \frac{1}{d+\beta V_0}e^{t(a+\beta V_0)}\right)v(a,t)
\end{aligned}
$$

Again, differentiation on both sides gives

$$
\begin{aligned}
\frac{\partial^3 v}{\partial t^3}(a,t) &= -u\frac{\partial^2 v}{\partial t^2}(a,t) - K\beta\lambda a(a+\beta V_0)\\
&\quad\times \left(\frac{\beta V_0}{d^2+d\beta V_0}e^{(a-d)t} + \frac{1}{d+\beta V_0}e^{t(a+\beta V_0)}\right)v(a,t)\\
&\quad + K\beta\lambda a\big(1+(-a-\beta V_0)t\big)\\
&\quad\times \left(\frac{\beta V_0}{d^2+d\beta V_0}e^{(a-d)t} + \frac{1}{d+\beta V_0}e^{t(a+\beta V_0)}\right)\frac{\partial v}{\partial t}(a,t)\\
&\quad - K\beta\lambda a(a+\beta V_0)\left(\frac{\beta V_0}{d^2+d\beta V_0}e^{(a-d)t} + \frac{1}{d+\beta V_0}e^{t(a+\beta V_0)}\right)v(a,t)\\
&\quad + K\beta\lambda a\big(1+(-a-\beta V_0)t\big)\\
&\quad\times \left(\frac{(a-d)\beta V_0}{d^2+d\beta V_0}e^{(a-d)t} + \frac{a+\beta V_0}{d+\beta V_0}e^{t(a+\beta V_0)}\right)v(a,t)
\end{aligned}
$$

Summarizing, we have

$$\begin{aligned}
&\frac{\partial^3 v}{\partial t^3}(a,t) + u\frac{\partial^2 v}{\partial t^2}(a,t) - K\beta\lambda a\big(1+(-a-\beta V_0)t\big) \\
&\quad\times\left(\frac{\beta V_0}{d^2+d\beta V_0}e^{(a-d)t} + \frac{1}{d+\beta V_0}e^{t(a+\beta V_0)}\right)\frac{\partial v}{\partial t}(a,t) \\
&= -2K\beta\lambda a(a+\beta V_0)\left(\frac{\beta V_0}{d^2+d\beta V_0}e^{(a-d)t} + \frac{1}{d+\beta V_0}e^{t(a+\beta V_0)}\right)v(a,t) \\
&\quad + K\beta\lambda a\big(1+(-a-\beta V_0)t\big)\left(\frac{(a-d)\beta V_0}{d^2+d\beta V_0}e^{(a-d)t} + \frac{a+\beta V_0}{d+\beta V_0}e^{t(a+\beta V_0)}\right)v(a,t)
\end{aligned} \tag{A.5}$$

For each $a \in [a_1, a_2]$, the latter equation is a third-order ordinary differential equation with variable coefficients. Using standard Lipschitz-continuity arguments (see, for instance, Sect. 4.3 in Königsberger (2004)), it can be shown that for each $a \in [a_1, a_2]$, the initial-value problem (A.5), together with $v(a,0) = v_0(a)$, $\frac{\partial v}{\partial t}(a,0) = -uv_0(a) + Kay_0(a) + a^{-1}KS_0(a)$ and $\frac{\partial^2 v}{\partial t^2}(a,0) = -u(-uv_0(a) + Kay_0(a) + a^{-1}KS_0(a)) + K\beta\lambda a(\frac{\beta V_0}{d^2+d\beta V_0} + \frac{1}{d+\beta V_0})v_0(a)$ (which we assume to be continuous functions of a), must have a unique solution defined on some interval $[0, T_1] \subset [0, \infty)$ of positive length $T_1 \in \mathbb{R}_+$. Given that the coefficients of (A.5) are continuous functions of a (which can be interpreted as a parameter in the ODE (A.5) in the framework of a sensitivity analysis), all the solutions $v(a,t)$ must be continuous on $[a_1, a_2] \times [0, T_1]$ (see, for instance, Theorem 6.1 in Epperson (2007) and also Sect. 3.1.1 in Deuflhard and Bornemann (2008)). This family of solutions allows us to construct a local solution (defined on $[a_1, a_2] \times [0, T_1]$) of (4) by means of substitution of $v(a,t)$ into the expressions (A.1), (A.2), and (A.3). The procedure can be now repeated for a short time interval starting at T_1 yielding the next local solution. A global solution can be obtained by patching together the local solutions and letting $T_i \to 0$.

Appendix B: Numerical Solution of the Continuous-Virulence Model's Equations

To solve the system of equations (4) numerically, we discretized the "virulence-space" with an equidistant grid $G_n([0.05, 0.5])$ and approximated the integrals $\int_{a_1}^{a_2} v(\xi,t)\,d\xi \approx \sum_{j\in G_n([0.05,0.5])} \gamma_j v(j,t)$ and $\int_{a_1}^{a_2} \frac{1}{a^{-1}+b^{-1}} \min(a,b)(z(a,b,t) + z(b,a,t))\,db \approx \sum_{j\in G_n([0.05,0.5])} \gamma_j \frac{1}{a^{-1}+j^{-1}} \min(a,j)(z(a,j,t) + z(j,a,t))$ using a Newton–Cotes quadrature formula of seventh order (with weights γ_j). After this discretization step, we obtain, for each pair $(a,b) \in (G_n([0.05, 0.5]) \times G_n([0.05, 0.5]))$, the following system of ordinary differential equations:

$$\dot{x}(t) = \lambda - dx(t) - \beta x(t) \sum_{j\in G_n([0.05,0.5])} \gamma_j v(j,t)$$

$$\frac{dy}{dt}(a,t) = \beta x(t) v(a,t) - \beta y(a,t) \sum_{j \in G_n([0.05,0.5])} \gamma_j v(j,t) - a y(a,t)$$

$$\frac{dz}{dt}(a,b,t) = \beta y(a,t) v(b,t) - \min(a,b) z(a,b,t)$$

$$\frac{dv}{dt}(a,t) = K a y(a,t) + a^{-1} K \sum_{j \in G_n([0.05,0.5])} \left(\gamma_j \frac{1}{a^{-1} + j^{-1}} \times \min(a,j)\big(z(a,j,t) + z(j,a,t)\big) \right) - u v(a,t)$$

The resulting system of coupled ordinary differential equations is solved numerically.

References

Anderson, R. M., & May, R. M. (1982). Coevolution of hosts and parasites. *Parasitology*, *85*(Pt 2), 411–426.

Barnett, S., & Šiljak, D. D. (1977). Routh's algorithm: a centennial survey. *SIAM Rev.*, *19*(3), 472–489.

Boldin, B., & Diekmann, O. (2008). Superinfections can induce evolutionarily stable coexistence of pathogens. *J. Math. Biol.*, *56*(5), 635–672. doi:10.1007/s00285-007-0135-1.

Bonhoeffer, S., Lenski, R. E., & Ebert, D. (1996). The curse of the pharaoh: the evolution of virulence in pathogens with long living propagules. *Proc. Biol. Sci.*, *263*(1371), 715–721. doi:10.1098/rspb.1996.0107.

Bonhoeffer, S., May, R. M., Shaw, G. M., & Nowak, M. A. (1997). Virus dynamics and drug therapy. *Proc. Nat. Acad. Sci. USA*, *94*(13), 6971–6976. URL http://www.pnas.org/content/94/13/6971.abstract.

Bonhoeffer, S., & Nowak, M. A. (1994). Mutation and the evolution of virulence. *Proc. Biol. Sci.*, *258*(1352), 133–140.

Bremermann, H. J., & Thieme, H. R. (1989). A competitive exclusion principle for pathogen virulence. *J. Math. Biol.*, *27*(2), 179–190.

Bull, J. J. (1994). Virulence. *Evolution*, *48*(5), 1423–1437.

Bull, J. J., Millstein, J., Orcutt, J., & Wichman, H. A. (2006). Evolutionary feedback mediated through population density, illustrated with viruses in chemostats. *Am. Nat.*, *167*(2), E39–E51. doi:10.1086/499374.

Coombs, D., Gilchrist, M. A., & Ball, C. L. (2007). Evaluating the importance of within- and between-host selection pressures on the evolution of chronic pathogens. *Theor. Popul. Biol.*, *72*(4), 576–591. doi:10.1016/j.tpb.2007.08.005.

Cooper, V. S., Reiskind, M. H., Miller, J. A., Shelton, K. A., Walther, B. A., Elkinton, J. S., & Ewald, P. W. (2002). Timing of transmission and the evolution of virulence of an insect virus. *Proc. Biol. Sci.*, *269*(1496), 1161–1165. doi:10.1098/rspb.2002.1976.

Cushing, J. M. (1977). *Integrodifferential equations and delay models in population dynamics*. *Lecture notes in biomathematics*. New York: Springer.

Deuflhard, P., & Bornemann, F. (2008). *Numerische Mathematik: Vol. 2. de Gruyter Lehrbuch [de Gruyter Textbook]*. Berlin: de Gruyter (revised ed.). Gewöhnliche Differentialgleichungen [Ordinary differential equations].

Domingo, E. (Ed.) (2006). *Quasispecies: concepts and implications for virology*. *Current topics in microbiology and immunology*. Berlin, Heidelberg: Springer.

Domingo, E., & Holland, J. J. (1997). RNA virus mutations and fitness for survival. *Annu. Rev. Microbiol.*, *51*, 151–178. doi:10.1146/annurev.micro.51.1.151.

Eigen, M. (1971). Self-organization of matter and the evolution of biological macromolecules. *Naturwissenschaften*, *58*(10), 465–523.

Eigen, M., McCaskill, J., & Schuster, P. (1988). Molecular quasi-species. *J. Phys. Chem.*, *92*(24), 6881–6891.

Epperson, J. F. (2007). *An introduction to numerical methods and analysis*. New York: Wiley-Interscience (revised ed.).

Ewald, P. W. (1983). Host-parasite relations, vectors, and the evolution of disease severity. *Annu. Rev. Ecol. Syst.*, *14*, 465–485.

Frank, S. A. (1996). Models of parasite virulence. *Q. Rev. Biol.*, *71*(1), 37–78.

García-Arriaza, J., Ojosnegros, S., Dávila, M., Domingo, E., & Escarmís, C. (2006). Dynamics of mutation and recombination in a replicating population of complementing, defective viral genomes. *J. Mol. Biol.*, *360*(3), 558–572. doi:10.1016/j.jmb.2006.05.027. URL http://www.sciencedirect.com/science/article/B6WK7-4K1G466-6/2/0e0dded6dbae0dad0b454d2ff9395a7a.

Holland, J. J., Torre, J. C. D. L., & Steinhauer, D. A. (1992). RNA virus populations as quasispecies. *Curr. Top. Microbiol. Immunol.*, *176*, 1–20.

Jung, A., Maier, R., Vartanian, J., Bocharov, G., Jung, V., Fischer, U., Meese, E., Wain-Hobson, S., & Meyerhans, A. (2002). Recombination: multiply infected spleen cells in HIV patients. *Nature*, *418*, 144.

Königsberger, K. (2004). *Analysis 2* (5th ed.). Berlin, Heidelberg: Springer.

Korobeinikov, A. (2004). Global properties of basic virus dynamics models. *Bull. Math. Biol.*, *66*(4), 879–883.

Krakauer, D. C., & Komarova, N. L. (2003). Levels of selection in positive-strand virus dynamics. *J. Evol. Biol.*, *16*(1), 64–73.

Kryazhimskiy, S., Dieckmann, U., Levin, S. A., & Dushoff, J. (2007). On state-space reduction in multi-strain pathogen models, with an application to antigenic drift in influenza A. *PLoS Comput. Biol.*, *3*(8), e159. doi:10.1371/journal.pcbi.0030159.

Lenski, R. E., & May, R. M. (1994). The evolution of virulence in parasites and pathogens: reconciliation between two competing hypotheses. *J. Theor. Biol.*, *169*(3), 253–265.

May, R. M., & Nowak, M. A. (1994). Superinfection, metapopulation dynamics, and the evolution of diversity. *J. Theor. Biol.*, *170*(1), 95–114. doi:10.1006/jtbi.1994.1171.

Novella, I. S., Reissig, D. D., & Wilke, C. O. (2004). Density-dependent selection in vesicular stomatitis virus. *J. Virol.*, *78*(11), 5799–5804. doi:10.1128/JVI.78.11.5799-5804.2004.

Nowak, M., & May, R. (2000a). *Virus dynamics*. London: Oxford University Press.

Nowak, M. A. (2006). *Evolutionary dynamics*. Cambridge: The Belknap Press of Harvard University Press.

Nowak, M. A., & May, R. M. (1994). Superinfection and the evolution of parasite virulence. *Proc. Biol. Sci.*, *255*(1342), 81–89. doi:10.1098/rspb.1994.0012.

Nowak, M. A., & May, R. M. (2000b). *Virus dynamics. Mathematical principles of immunology and virology*. Oxford: Oxford University Press.

Ojosnegros, S., Beerenwinkel, N., Antal, T., Nowak, M. A., Escarmísa, C., & Domingo, E. (2010a). Competition–colonization dynamics in an RNA virus. *Proc. Natl. Acad. Sci. USA*, *107*(5), 2108–2112. doi:10.1073/pnas.0909787107.

Ojosnegros, S., Beerenwinkel, N., & Domingo, E. (2010b). Competition–colonization dynamics: an ecology approach to quasispecies dynamics and virulence evolution in RNA viruses. *Commun. Integr. Biol.*, *3*(4), 333–336.

Perelson, A., & Nelson, P. (1999). Mathematical analysis of HIV-1 dynamics in vivo. *SIAM Rev.*, *41*(1), 3–44.

Sanz-Ramos, M., Diaz-San Segundo, F., Escarmis, C., Domingo, E., & Sevilla, N. (2008). Hidden virulence determinants in a viral quasispecies in vivo. *J. Virol.*, *82*(21), 10,465–10,476. doi:10.1128/JVI.00825-08. URL http://jvi.asm.org/cgi/content/abstract/82/21/10465.

Tilman, D. (1994). Competition and biodiversity in spatially structure habitats. *Ecology*, *75*, 2–16.

De la Torre, J. C., & Holland, J. J. (1990). RNA virus quasispecies populations can suppress vastly superior mutant progeny. *J. Virol.*, *64*(12), 6278–6281.

Turner, P. E., & Chao, L. (1999). Prisoner's dilemma in an RNA virus. *Nature*, *398*(6726), 441–443. doi:10.1038/18913.